Orientational distributions and nematic order of rodlike magnetic nanoparticles in dispersions

V. V. Krishnamurthy
Neutron Scattering Sciences Division, Oak Ridge National Laboratory, Oak Ridge, Tennessee 37831-6430, USA

G. J. Mankey, B. He, M. Piao, J. M. Wiest, and D. E. Nikles
Center for Materials for Information Technology, The University of Alabama, Tuscaloosa, Alabama 35487-0209, USA

L. Porcar
NIST Center for Neutron Research, National Institute of Standards and Technology, Gaithersburg, Maryland 20899-8562, USA

J. L. Robertson
Neutron Scattering Sciences Division, Oak Ridge National Laboratory, Oak Ridge, Tennessee 37831-6393, USA
(Received 1 May 2007; revised manuscript received 6 December 2007; published 13 March 2008)

Using small-angle neutron scattering (SANS), we have investigated the orientational order of iron nanoparticles dispersed in cyclohexanone. The particles have rodlike shape and size distributions with an average length of 200 nm and an average diameter of 25 nm. SANS shows an anisotropy, which is a measure of orientational order, in magnetic dispersions with a volume fraction of 3.2% and 3.9% iron particles in shear flow and/or magnetic field. The scattering anisotropy can be fitted by a model assuming an Onsager distribution of the orientation of the particles in shear flow. The orientational distribution of particles oriented by a magnetic field can be described by a different model assuming the Maier-Saupe orientational distribution for uniaxial ferromagnetic particles. The orientational distribution parameter m for the Maier-Saupe distribution or α for the Onsager distribution and the orientational order parameter S have been determined at shear rates $\dot{\gamma}$ of to $0-4000\ \mathrm{s}^{-1}$ and in magnetic fields of 0–18 mT. The S values indicate that the particles start to orient either in a shear flow of $100\ \mathrm{s}^{-1}$ or in a magnetic field of 6 mT. Applying only shear results in an orientational order, with the dispersion returning to the disordered state when the shear rate is decreased to zero. In sharp contrast, application of magnetic fields greater than 6 mT results in orientational order in the field-increasing cycle, and two-thirds of the orientational order remains when the field is decreased to zero. This shows that the order in a magnetic field is different from the order in a shear flow, the action of magnetizing the particles along a certain direction is irreversible, and the orientational order parameter exhibits hysteresis.

DOI: 10.1103/PhysRevE.77.031403 PACS number(s): 82.70.−y, 75.50.Mm, 83.50.Ax, 28.20.Cz

I. INTRODUCTION

Magnetic fluids such as magnetic dispersions and magnetic inks are heterogeneous, because they are mixtures of small particles and a solvent. The macroscopic mechanical properties of magnetic fluids (the storage modulus, for example) are completely different from those of their constituent phases. They also exhibit novel rheological properties in shear flows and in electric and magnetic fields [1]. Due to these properties, magnetic fluids have novel applications, such as mechanical position controllers in automobiles and as magnetic tape coatings for high-density data storage [2]. The orientational order of nanometer to micrometer sized acicular particles in dispersions and suspensions has attracted considerable interest [3,7]. Dispersions of such particles that are ferromagnetic offer the possibility of orienting them in a specific direction due to their shape anisotropy. The suitability of nanoparticles for magnetic recording applications depends on the ability to control their orientational order using an external force field, such as a shear flow or a magnetic field. The rheological properties of such magnetic particle dispersions therefore strongly depend on the size and shape of the particles, the size distribution, and the interparticle interactions. Typically, the magnetic particles used for tape coatings have a log-normal size distribution and the dispersions exhibit shear-thinning behavior. It is desirable to have a quantitative measure of the degree of orientational order and the dynamics of magnetic particles in a dispersion when subjected to shear and magnetic fields, which are used to orient the particles during the fabrication of magnetic tape.

Detailed studies of the influence of particle size, polydispersity, and concentration of particles on the shear-induced alignment of anisotropic particles in dispersions and suspensions are of common interest for a wide range of applications [4]. Small-angle neutron scattering (SANS) in combination with a Couette shear cell is a suitable technique to investigate the shear-induced structures in complex fluids [5]. SANS has been successfully used to investigate shear-induced effects such as association, breaking, and alignment of cylindrical micelles in solutions [6]. SANS measurements show that shear-flow-induced alignment of micrometer sized, anisotropic, precipitated calcium carbonate particles in shear-thickening suspensions increases with the particle aspect ratio and shear stress [7]. In our earlier experiments, we have also applied SANS to detect orientational order in a magnetic dispersion of iron nanoparticles having an average aspect ratio of 8 (average length of 200 nm and average diameter of 25 nm) in cyclohexanone [3]. These experiments, performed on a dispersion with a volume fraction of 4.4% iron nanoparticles in cyclohexanone, showed that particles with size polydispersity could be aligned along the shear flow or along the magnetic field. Applying the shear in the presence of a

magnetic field results in a change of orientation of the particles from a field-aligned to a shear-aligned state. A single-particle mean-field model [3,8,9] that takes into account particle Brownian motion, anisotropic hydrodynamic drag, a steric potential, and magnetic dipolar interaction showed qualitative agreement with the experimental results. A more accurate determination of the order parameter rather than the anisotropy in the SANS pattern under different conditions of shear flow and magnetic field is necessary for a quantitative treatment as well as a better understanding of the orientational order as a function of the applied magnetic field and shear rate $\dot{\gamma}$. In this paper, we report the orientational distributions and orientational dynamics of magnetic dispersions in Couette shear flow and magnetic field from small-angle neutron scattering experiments. The dispersions consist of (a) 3.2% and (b) 3.9% volume fractions of cylindrical shaped iron nanoparticles with cyclohexanone as solvent. The modeling of the SANS intensity, using Onsager orientational distributions for shear-induced order and Maier-Saupe orientational distributions for field-induced order, enabled us to accurately determine the order parameter in the dispersions as a function of shear rate and/or magnetic field. Such quantitative information on the degree of the orientational order in a dilute magnetic dispersion in shear flow and/or magnetic field can in general be useful for understanding how orientational order develops in dispersions containing magnetic nanoparticles with size polydispersity.

This paper is organized as follows. The properties of Fe nanoparticles and the SANS experimental set-up are briefly described in Sec. II. SANS experimental results, the data analysis, and the discussion of results are presented in Sec. III. Finally, a summary of the present SANS investigations is given in Sec. IV.

II. EXPERIMENT

The iron particles used in our dispersions have the following properties: saturation magnetization of 120 A m^2/kg, coercivity of 130–220 mT, specific surface area of 42 000 m^2/kg, average length of 200 nm, average aspect ratio of 8, and density of 5700 kg/m^3. They have a log-normal length distribution that has a width of 20%. The magnetic dispersions were prepared using cyclohexanone as a solvent, a commercial antiflocculating polymer MR110 (Nippon Zeon Co.), and iron metal particles, following the procedure reported in Ref. [3]. Adsorption of the MR110 polymer onto the particle surfaces provides steric stabilization against agglomeration. Cyclohexanone was chosen as the solvent because it is a good solvent for MR110 and it has low volatility. Small-angle neutron scattering from the dispersions was measured using the 30 m NG3 SANS instrument at the NIST Center for Neutron Research, Gaithersburg, Maryland. The experimental setup consists of a Couette shear cell that has the shear flow in the x direction [10] and a Helmholtz coil that produces a field of 18 mT along the z direction, i.e., perpendicular to the plane of shear flow. A schematic of the experimental setup can be found in Ref. [3]. Neutrons of 0.6 nm wavelength and a sample-to-detector distance of 13.1 m were chosen to cover the values of the horizontal scattering vector $q=4\pi \sin\theta/\lambda$, where θ is the scattering angle, in the range of $0.044-0.34$ nm^{-1}. The shear rate $\dot{\gamma}$ is given by $\partial v_x/\partial y$, where v_x is the flow velocity. Neutrons were incident on the sample along the y direction. The magnetic field is applied along the vertical (z) direction, i.e., in the vorticity direction. Scattered neutrons were detected in the x-z plane by an area-sensitive detector.

The measurements were performed under different experimental conditions of shear and/or magnetic field. For each measurement, the SANS intensity data were collected as two-dimensional contour plots in the q_x-q_z plane. Each data set was corrected for detector background, detector sensitivity, scattering from the empty cell, and transmission, and the intensity was scaled to absolute units of cross section per unit volume as is done in conventional SANS data reduction. We define ψ as the angle between the direction of q and the positive q_x axis. The scattered neutron intensity $I(\psi)$, which is a function of the azimuthal angle ψ, is obtained by integrating the scattered neutron counts at the scattering vector $q=0.08$ nm^{-1} with $dq=0.0045$ nm^{-1} using the NIST SANS data reduction program [11]. $I(\psi)$ was first obtained for different values of the scattering vector and the results compared. Qualitatively, they are the same for all q values. We have chosen $q=0.08$ nm^{-1} over the other values because it yields better azimuthal resolution in addition to a high signal-to-noise ratio. $I(\psi)$ thus obtained has two contributions: one is the scattering by the nanoparticles and the other by the solvent. The contribution from the solvent is isotropic and does not depend on either the shear rate or the magnetic field. Note that 75% of the scattering length density contrast of the iron nanoparticles arises from the nuclear contribution and the remaining 25% arises from the magnetic contribution [12,13]. Since the magnetic moment and the magnetization easy axis of the particle are expected be to along its long axis, both the contributions give a measure of the orientation of the particle in the dispersion.

III. RESULTS AND DISCUSSION

A. Scattering vector dependence of SANS intensity: Particle size estimate

In general, the scattering intensity $I(q)$, where q is the magnitude of the scattering vector, is proportional to the SANS differential cross section and is given by [14]

$$I(q) = N_P V_P^2 P(q) S(q) + B_G, \tag{1}$$

where N_P is the number density of the scattering centers, V_P is the volume of one concentration center, $P(q)$ is known as the particle form factor or shape factor, $S(q)$ is the interparticle structure factor, and B_G is a constant background. Therefore, $I(q)$ contains information on the shape, the size, and the interaction(s) between the scattering centers in the dispersion. Therefore, by modeling $P(q)$ and $S(q)$ one can obtain information on the particle sizes and the interparticle interactions, respectively. The magnetic contribution is zero on average, as the particles are randomly oriented. In a dispersion with a volume fraction of 3–4 % Fe particles, there may be some hard sphere repulsion i.e., a small contribution

from the structure factor. However, this contribution is expected to be at lower q values. Here we are mostly interested in the high-q range where we can model the scattering intensity with the form factor. Therefore, for dilute particle concentrations and randomly oriented particles, the structure factor $S(q)$ at high q can be taken as unity.

For cylindrically shaped core-shell particles of length L, core radius r, and shell thickness t, the single-particle form factor is given by [15]

$$F(q,\gamma) = 2(\rho_{\text{core}} - \rho_{\text{shell}})V_{\text{core}} j_0\left(\frac{qL}{2}\cos\gamma\right)\frac{J_1(qr\sin\gamma)}{qr\sin\gamma} + 2(\rho_{\text{shell}} - \rho_{\text{solvent}})V_{\text{shell}} j_0\left[q\left(\frac{L}{2}+t\right)\right] \times\cos\gamma\left]\frac{J_1[q(r+t)\sin\gamma]}{q(r+t)\sin\gamma}\right., \quad (2)$$

where γ is the angle between the cylinder axis and scattering vector q. Here $V_{\text{core}} = \pi r^2 L$ is the volume of the particle core, ρ_{core} is the neutron scattering length density (NSLD) of the core, ρ_{shell} is the NSLD of the shell, which is a polymer, ρ_{solvent} is the NSLD of the solvent, $j_0(x) = \sin(x)/x$, and $J_1(x)$ is the first-order Bessel function of x. The polydispersity of the radius p of the particles is defined as $(\langle r^2\rangle - \langle r\rangle^2)/\langle r\rangle$.

The scattering intensity is calculated by first doing an orientational average over the cylinder form factor, which is then averaged over a log-normal distribution of the cylinder radius r [11]. Polydispersity in particle size results in damping of the oscillations in the form factor at high q values [15–17]. The polydispersity of the radius p is thus included by integrating the cylinder form factor $P(q)$ over a log-normal distribution of cylinder radius, and the integration is normalized by the second moment of the radius distribution. The scattering intensity per unit volume is given by

$$I(q) = \phi\bar{P}(q), \quad (3)$$

where ϕ is the particle volume fraction and $\bar{P}(q)$ is the size-averaged form factor. $\bar{P}(q)$ is given by

$$\bar{P}(q) = \frac{1}{V_{\text{poly}}}\int_0^x P(q)f(r)dr, \quad (4)$$

where $P(q)$ is the orientation-averaged form factor of a cylinder of length L and radius r for the Couette shear cell geometry [6,18–22], $f(r)$ is the log-normal distribution of the radius, and V_{poly} is the polydispersity volume. $P(q)$ is given by

$$P(q) = \frac{\text{const}}{V_{\text{tot}}}\int_0^{\pi/2} F(q,\gamma)^2\sin\gamma\, d\gamma, \quad (5)$$

where "const" is the proportionality factor, and $V_{\text{tot}} = \pi(r+t)^2(L+t)$ is the volume of the core and the shell, with t being the shell thickness. The best fit to this model, displayed as a solid line in Fig. 1(a), yielded the diameter $2r = 21 \pm 2$ nm, length $L = 229 \pm 30$ nm, a shell of ~ 2 nm, and the polydispersity of the radius $p \sim 0.4$. Therefore, fitted values of the diameter of the particle including the shell

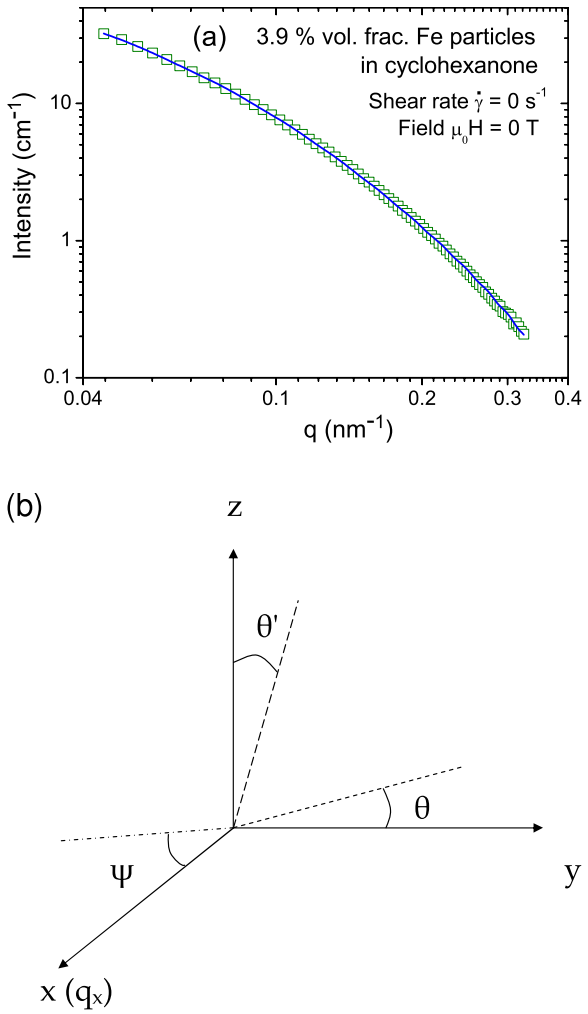

FIG. 1. (Color online) (a) Scattering vector q dependence of the SANS intensity $I(q)$ in 3.9 vol. % iron nanoparticle dispersion. The error bars are equal to one standard deviation. The solid line is the best fit to the q dependence of scattering intensity using the form factor of core-shell cylinders with polydispersity in the radius, defined by Eqs. (1)–(5). (b) Illustration showing the definition of angles θ, θ', and ψ with respect to the Cartesian coordinate axes.

25 ± 2 nm and the length of 233 ± 30 nm compare quite well with the average sizes ($2r \sim 25$ nm, and $L \sim 200$ nm) of the particles.

B. Model for the anisotropic scattering and orientational order

1. Orientational order of particles in shear flow

Computer simulations show that finite-length hard rods, such as the iron nanoparticles used in our dispersions, show liquid crystalline phases, namely, a nematic phase, a smectic phase, and a columnar phase [23]. Nematic phase transitions are reported at aspect ratio values such as 15 [24]. In the nematic phase, the particles exhibit long-range orientational order, without a translational order. The orientational order of nanoparticles in our dispersions can be best described by the nematic phase. For this purpose, we choose a preferred di-

rection (the vorticity direction in the shear flow or the direction of the magnetic field), i.e., the director. We define the angle between the particle long axis and the z axis as θ' [see Fig. 1(b)]. Therefore, θ' is the angle between the particle long axis and the director (z axis) for orientational order in the magnetic field. Then, $\pi/2-\theta'$ is the angle between the particle long axis and the director, which is in the xy plane, for orientational order in shear flow. The nematic order is often characterized by the orientational distribution function (ODF) $f(\theta')$, which is a single-particle distribution function. It describes the distribution of orientations of the particles about a preferred direction, i.e., the director.

For the nematic order of iron nanoparticles in the dispersion, the Onsager orientational distribution function [25] can be written as

$$f(\theta') = \frac{\alpha \cosh[\alpha \cos(\pi/2 - \theta')]}{\sinh(\alpha)}, \tag{6}$$

where α is the distribution parameter. Then the nematic order parameter S of a system is quantified by

$$S = \int_0^{\pi/2} d(\pi/2 - \theta')\{\sin(\pi/2 - \theta')P_2[\cos(\pi/2 - \theta')]f(\theta')\}, \tag{7}$$

where $P_2(x)$ is the Legendre polynomial of variable x. Recently, Savenko and Dijkstra developed a formalism for determining the nematic order parameter S and orientational distribution function from small-angle scattering [26]. In their approach, the small-angle scattering intensity as a function of the angle ψ, which is the angle with the positive q_x axis of the SANS two-dimensional (2D) plot, can be related to the ODF $f(\theta')$ using the Leadbetter formula [26,27]. q_x is parallel to the x axis in our notation, which is shown in Fig. 1(b). If we consider the Onsager ODF, defined above, for $f(\theta')$, then we get [24]

$$I(\psi) = I_c \frac{\alpha}{\sinh(\alpha)}[1 + (\pi/2)L_1(\alpha \sin \psi)], \tag{8}$$

where $L_1(z)$ is the modified Struve function of z of order 1 and is defined as [28]

$$L_1(z) = \frac{z}{\sqrt{\pi}\Gamma(3/2)} \int_0^{\pi/2} \sinh[z \cos(\theta')] \sin^2(\theta') d\theta', \tag{9}$$

and I_c is a proportionality constant. The intensity at $\psi=0$ is given by $I(0)=I_c\alpha/\sinh(\alpha)$.

Figure 2 shows the azimuthal angle dependence of the neutron scattering intensity $I(\psi)$ in the two dispersions with volume fractions of 3.2% and 3.9% iron nanoparticles at selected shear rates in the range of $0-4000$ s^{-1} in zero applied field. The intensity is isotropic when the dispersion is at zero shear rate in zero applied field as the particles are randomly oriented in the absence of an external torque. When the dispersion is subjected to shear flow, the scattering intensity develops sinusoidal oscillations above a characteristic shear rate with maxima at $\psi=90°$ and $\psi=270°$, i.e., along the q_z direction. The anisotropy in intensity is a clear indication

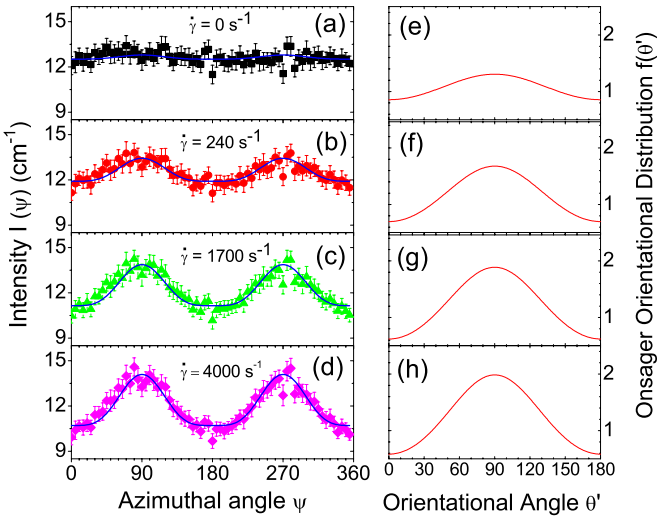

FIG. 2. (Color online) (a)–(d) Neutron scattering intensity as a function of the azimuthal angle in the 3.9% volume fraction iron nanoparticle dispersion at selected shear rate $\dot{\gamma}$ of 0, 240, 1700, and 4000 s^{-1} in zero applied magnetic field. The solid lines in (a)–(d) are the best fits by Eq. (8). (e) and (h) show the Onsager orientational distribution of the nanoparticles for the α values of fitted curves shown in (a) and (d).

of orientational order of the nanoparticles and the formation of a nematic phase. With increasing shear rate, the amplitude of the oscillations increases monotonically. The solid lines in Fig. 2 are best fits by Eq. (8).

The intensity $I(\psi)$ for this case could be fitted best with Eq. (8), to determine $I(0)$ and α. The values of α and the order parameter S for the shear-rate-increasing cycle are plotted as a function of shear rate in Fig. 3. With increasing shear rate, α increases monotonically from about 1.125 at 10 s^{-1} (7 s^{-1}) in the dispersion with 3.2% (3.9%) volume fraction iron nanoparticles to about 1.87 at 4000 s^{-1}. At low shear rates, individual particles align in the flow with their long axis along the direction of flow. The change in the slope of S at a shear rate 100 s^{-1} indicates that particles start to orient collectively in the flow. The values of α and S are nearly the same for the two volume fractions of the particles in the dispersion.

2. Orientational order of particles in magnetic field: Hysteresis behavior

In the presence of a magnetic field, the steric interaction and the dipolar interaction between the magnetic particles are also expected to play a role in the orientational order. In the absence of shear flow, the orientational distribution of particles induced by the magnetic field can be described by the orientational distribution function of uniaxial ferromagnetic particles [1], which is similar to the Maier-Saupe orientational distribution function [24,27]

$$f(\theta') = \frac{1}{Z}\exp(m \cos^2 \theta'), \tag{10}$$

where m is a parameter related to the order parameter S of the particle, and Z is the normalization constant such that

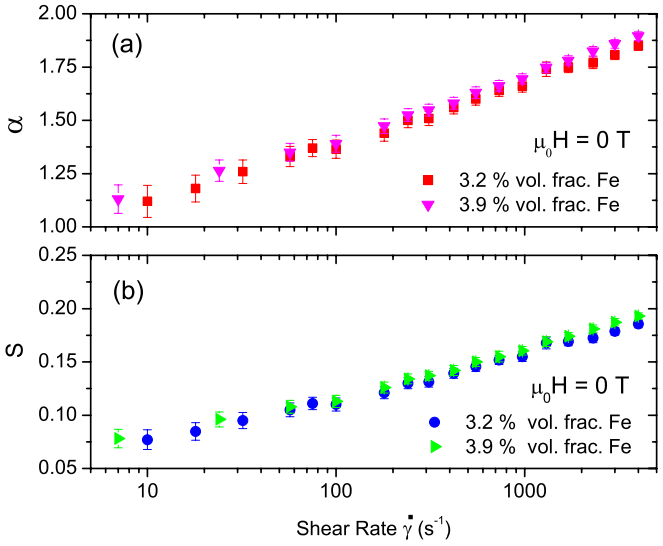

FIG. 3. (Color online) (a) Onsager orientational distribution parameter α and (b) nematic order parameter S as functions of shear rate for the dispersion at the two (3.2% and 3.9%) volume fractions of iron nanoparticles in zero applied field. Filled circles indicate the shear-rate-increasing cycle, and open circles indicate the shear-rate-decreasing cycle. Increase of S indicates particle alignment along the flow.

$\int_0^{\pi/2} d\theta' \sin\theta' f(\theta') = 1$. From this normalization integral, we obtain the relation between Z and m as

$$Z = \frac{1}{2\sqrt{m}} \sqrt{\pi}\, \mathrm{erfi}(\sqrt{m}), \tag{11}$$

where $\mathrm{erfi}(x)$ is the imaginary error function of variable x.

Then the nematic order parameter S of a system is quantified by

$$S = \int_0^{\pi/2} d\theta' (\sin\theta') P_2(\cos\theta') f(\theta'), \tag{12}$$

where $P_2(x)$ is the Legendre polynomial of variable x.

The small-angle scattering intensity as a function of the angle ψ, the angle with the positive q_x axis of the SANS 2D plot, is related the Maier Saupe ODF $f(\theta')$ by the following equation [27]:

$$I(\psi) = I_b + \frac{\exp(m\cos^2\theta')}{\sqrt{m} Z \cos\theta'} \frac{\pi}{2} \mathrm{erf}(\sqrt{m}\cos\theta'), \tag{13}$$

where I_b is the q-independent scattering contribution and $\mathrm{erf}(x)$ is the error function of variable x. Note that the SANS experiments were always performed at a steady shear flow. We define the shear-rate-increasing cycle as the set of measurements in which the shear rate of a particular scan was higher than the shear rate of the previous scan. Similarly, the shear-rate-decreasing cycle is defined as the set of measurements in which the shear rate of a particular scan was lower than that of the previous scan.

Experiments on the dispersion with a volume fraction of 3.2% iron nanoparticles in the field-increasing and field-decreasing cycles were conducted under conditions of zero shear rate to investigate the field dependence of the orientational order in the dispersion. Figure 4 shows the SANS intensity as a function of the azimuthal angle in the dispersion with a 3.2% volume fraction of iron nanoparticles in a magnetic field of 18 mT at zero shear rate. The scattering intensity at all field values could be fitted with Eq. (13). Figure 4(b) shows the orientational distribution as a function of the orientational angle for the m value returned by the fit shown in Fig. 4(a). The distribution parameter m extracted from the best fits and the resulting order parameter S are shown in Fig. 5 for the dispersions with volume fractions of 3.2% and 3.9% iron nanoparticles as functions of applied magnetic field. In the field-increasing cycle, the anisotropy is negligible below a characteristic field value of 6 mT; therefore there is no evidence for orientational order in the dispersion. The anisotropy in the scattering appears in fields greater than or equal to 6 mT in this cycle. The anisotropy of the scattering intensity increases with the field as the number of particles ordering in the field increases. The parameter m increases with further increase of the applied field and satu-

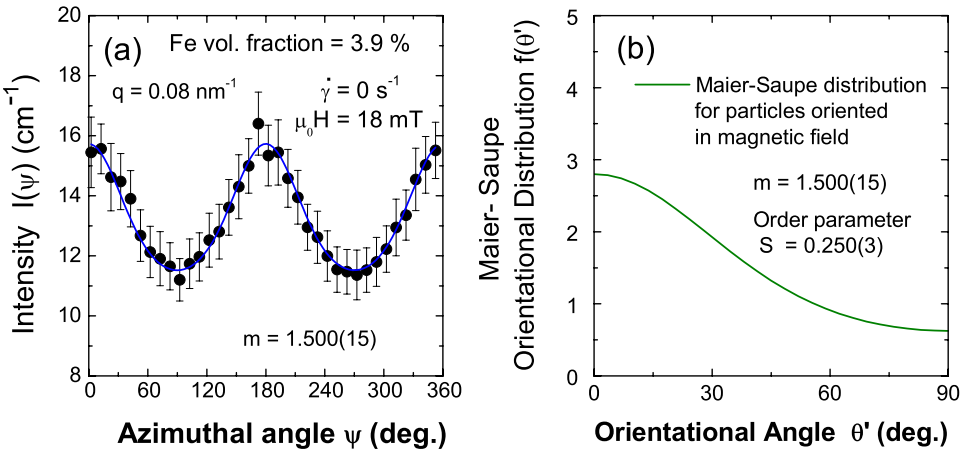

FIG. 4. (Color online) (a) Neutron scattering intensity as a function of the azimuthal angle in the 3.2% volume fraction iron nanoparticle dispersion in a magnetic field of 18 mT at zero shear rate. The solid lines are the best fits by Eq. 14. (b) Maier-Saupe orientational distribution of the nanoparticles for the m values of the fitted curve in (a).

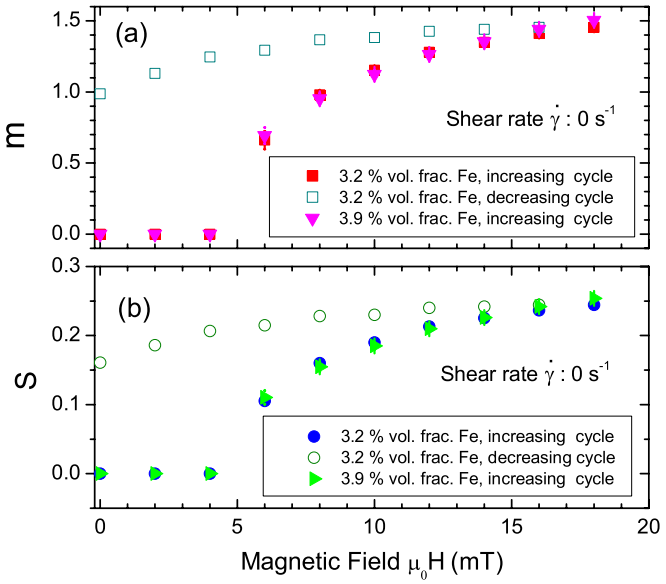

FIG. 5. (Color online) Magnetic field dependence of Maier-Saupe distribution parameter m and order parameter S in 3.2% and 3.9% volume fraction Fe nanoparticle dispersions.

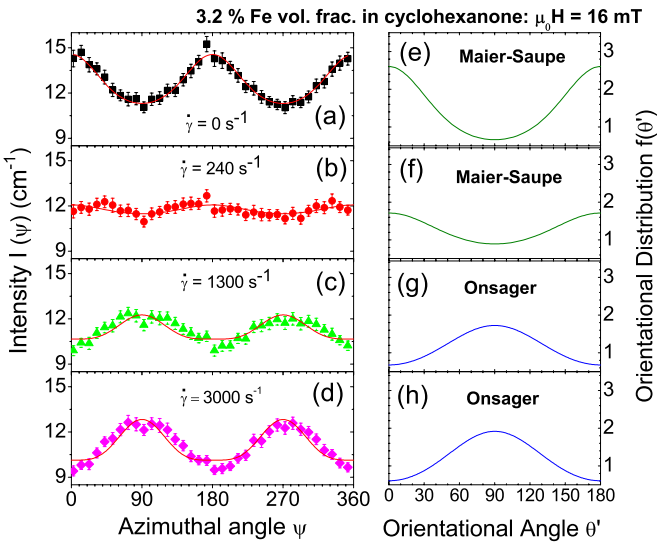

FIG. 6. (Color online) (a)–(d) Neutron scattering intensity as a function of the azimuthal angle in the 3.2% volume fraction iron nanoparticle dispersion at selected shear rate $\dot{\gamma}$ of 0, 240, 1300, and 3000 s^{-1} in a magnetic field of 16 mT. The solid lines in (a) and (b) are the best fits by Eq. (13) and those in (c) and (d) are best fits by Eq. (8). (e) and (h) show the orientational distribution of the nanoparticles for the α values of fitted curves shown in (a) and (d).

rates at a value of about 1.45 in the 3.2 vol % dispersion (1.5 in the 3.9 vol % dispersion) in a field of 18 mT.

The value of S also increases with the applied field. The m and S values in the dispersion with a volume fraction of 3.9% iron nanoparticles are very similar to those found in the dispersion with a volume fraction of 3.2% iron nanoparticles, suggesting that the small increase in the particle concentration does not change the degree of orientational order. When the field is reduced from 18 to 0 mT along the same values, m and S are found to be higher suggesting hysteresis behavior in the ordering below a characteristic value of the field $\mu_0 H_C \leq 14$ mT. When the field is switched off, the particles maintain a considerable degree of the orientational order induced by the field. These features suggest that a greater number of particles order in the field-decreasing cycle for a given value of magnetic field.

Onsager has suggested that particle agglomeration can occur in particle dispersions due to a steric interaction between the particles [29]. Since the particle volume fractions used in our dispersions are much lower than the necessary value of 50% for phase separation in a dispersion of particles having an axis ratio of 8, we conclude that the agglomeration does not occur through steric interaction. However, agglomeration can occur in dispersions containing small volume fractions of acicular (needlelike) magnetic particles through magnetic interaction. Cebers has shown that magnetic interactions can lead to the formation of anisotropic aggregates with antiferromagnetic ordering of magnetic particles at small volume fractions [30]. Models based on agglomeration in the presence of a magnetic field have been developed to explain the ordering properties of magnetic fluids [31]. We believe that the agglomeration process occurring in our dispersions is driven by magnetic interactions, in particular, the dipolar interaction. The irreversibility of the order parameter with the field indicates that the particles mutually induce dipole moments even when the field is reduced to zero and attractive forces between the particles dominate over the repulsive forces. The attractive forces between the particles support the possibility of antiferromagnetically aligned agglomerates at zero or low fields.

The applied magnetic field can change the alignment of particles from an antiferromagnetic to a ferromagnetic configuration in some of the agglomerates and this can result in the increase of the order parameter S. Morozov has theoretically shown that needlelike ferromagnetic agglomerates are thermodynamically more favorable than droplike antiferromagnetic agglomerates in the presence of an applied magnetic field [31]. Our results qualitatively support some of the predictions of this theory. Because the magnitude of S found in the experiment is much less than 1, which is expected for perfect order such as ferromagnetic alignment of particles along the field direction, it is likely that there is significant antiferromagnetic order of particles in the agglomerates even at the highest applied field of 18 mT. Therefore, the reduction of the magnitude of S from the ideal value of 1 can qualitatively account for partial antiferromagnetic order within the agglomerates.

C. Orientational ordering of particles in magnetic field and shear flow

Figure 6 shows plots of neutron scattering intensity as a function of the azimuthal angle in the dispersion with a volume fraction of 3.2% iron nanoparticles in a field of 16 mT at selected shear rates. As seen in Fig. 5(a), when the shear rate is nearly zero and a magnetic field of 16 mT is applied along the z direction, the scattering intensity is strongly oscillatory with maxima in the intensity at ψ=0°, 180°, and 360°, i.e., in the q_x-q_y plane. The location of the maxima in

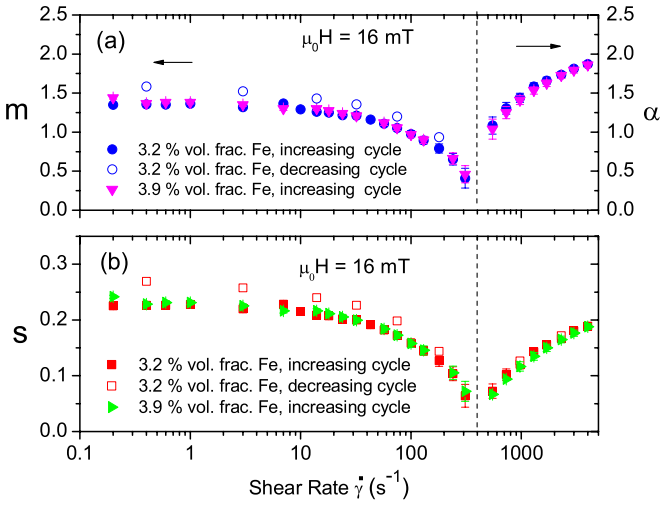

FIG. 7. (Color online) Shear rate $\dot{\gamma}$ dependence of (a) the Maier-Saupe distribution parameter m and Onsager orientational distribution parameter α and (b) the nematic order parameter S in the dispersions at 3.2% and 3.9% volume fraction iron nanoparticle concentrations in a field of 16 mT. Filled circles indicate the shear-rate-increasing cycle, and open circles indicate the shear-rate-decreasing cycle. The minimum in S indicates the loss of orientational order due to the balance of the torques due to the field and shear flow.

the reciprocal space implies orientational order along the z direction in real space, i.e., along the direction of the magnetic field. As the dispersion is sheared under the influence of a magnetic field, the amplitude of the oscillations in the scattering intensity decreases with increase of the shear rate and vanishes at a characteristic shear rate of 420 s^{-1}, indicating a reduction in the degree of orientational order in the field, i.e., a decrease in the number of particles of the dispersion ordered along the field.

The orientational order in the dispersion under the simultaneous action of the shear flow and the field for all the values of magnetic field and shear rate can be described by a biaxial orientational distribution, which has one director in the direction of the magnetic field, i.e., along the z direction, and the other director in the shear flow, i.e., in the x-y plane. Our experimental data indicate that the shape of the SANS intensity curves goes through a transition at about a characteristic shear rate of 420 s^{-1} in a field of 16 mT. Considering this feature in the data, we make the approximation that the orientational order of the dispersion is predominantly in the magnetic field below a characteristic value of the shear rate and use the uniaxial distribution defined by Eq. (10). Similarly, we make the approximation that the orientational order of the dispersion is predominantly in the shear flow, i.e., x-y plane, above the characteristic value of the shear rate and use the Onsager distribution defined by Eq. (6).

We find that Eq. (13) in fact fits the intensity for shear rate less than 420 s^{-1} quite well. Figure 7 shows the shear rate dependence of m in Fig. 7(a) and S in Fig. 7(b) for the dispersion with a volume fraction of 3.2% iron nanoparticles in the shear-rate-increasing and -decreasing cycles together with the values for the dispersion with a volume fraction of 3.9% iron nanoparticles in the shear-rate-increasing cycle. The parameter m decreases from about 1.37 in the rate-increasing cycle (1.58 in the rate-decreasing cycle) at a shear rate of 0.4 s^{-1} to 0.46 at a shear rate of 310 s^{-1}. The order parameter S has the highest value at 0 s^{-1}. It gradually decreases with increase of the shear rate and vanishes at about a shear rate of 420 s^{-1}. Therefore, when the shear rate is less than or equal to 310 s^{-1}, we expect that the long axes of the particles that are ordered in the field remain parallel to the magnetic field. Near a characteristic shear rate of 420 s^{-1}, the order parameter S is close to zero, indicating random orientation or disorder in the dispersion due the cancellation of the field-induced and the flow-induced torques on the nanoparticles.

When the shear rate exceeds the characteristic value of 420 s^{-1}, the anisotropy in the scattering increases with the shear rate and the scattering pattern shows resemblance to the pattern observed in the shear-only condition as the torque of the shear flow starts to dominate over the torque induced by the magnetic field [see Figs. 6(c) and 6(d)]. This is the case when the particle long axis is in the q_x-q_z plane, i.e., in the plane of shear flow. The parameters α and S give a measure of the degree of orientational order of nanoparticles in the dispersion in shear flow. We find that Eq. (6) gives a good description of the azimuthal angle dependence of $I(\psi)$ in this high-shear-rate region. The values of α and S returned by the best fits are also shown in Fig. 6. Both α and the magnitude of S increase with the shear rate and recover to their highest values at a shear rate of 4000 s^{-1}, indicating that the torque induced by the shear flow on the particles completely dominates the torque due to the magnetic field on the particles.

The SANS experiments in the dispersion with a volume fraction of 3.2% iron nanoparticles were performed in both the shear-rate-increasing and the shear-rate-decreasing cycles to study the reversibility of orientational order. In the shear-rate-decreasing cycle, the anisotropy is found to be larger than the values observed at the corresponding shear rate in the shear-rate-increasing cycle, indicating irreversibility of the number of ordered particles. But the characteristic shear rate for the crossover of field-induced to shear-induced order remains at 420 s^{-1}. The larger values of anisotropy in the shear-rate-decreasing cycle could result from slow orientation of larger-sized particles and the particle agglomerates in the dispersion by the magnetic field, resulting in an increase of the number of oriented particles. Irreversibility is also clearly seen in the shear rate dependence of m, α, and S values of the dispersion with a volume fraction of 3.2% iron nanoparticles in Fig. 7.

IV. SUMMARY

Small-angle neutron scattering experiments have been performed on rod shaped iron nanoparticle dispersions having volume fractions of 3.2% and 3.9% in cyclohexanone under different conditions of shear and applied magnetic field. The anisotropy of small-angle neutron scattering intensity observed in the case of shear-flow-induced order has been modeled by considering Onsager orientational distribution functions of particles in shear flow. The anisotropy of

the SANS intensity observed in the case of particles oriented in the magnetic field can be described by the orientational distribution of uniaxial ferromagnetic particles or the Maier-Saupe distribution. The analysis helps us to directly determine the degree of orientational order in terms of the Onsager orientational distribution parameter α or the Maier-Saupe orientational distribution parameter m, and the orientational order parameter S in the dispersions. The trends observed in the shear rate and magnetic field dependence of α and S show that magnetic nanoparticles (average length 200 nm, average diameter 25 nm) with polydispersity in length and/or diameter can be aligned either in a shear flow or in a magnetic field above a characteristic value of the shear rate $\dot{\gamma} \approx 100\ \mathrm{s}^{-1}$ or a characteristic value of the magnetic field of 6 mT. The characteristic value of the shear rate or the magnetic field or the degree of order is nearly independent of the volume fraction in the investigated range of 3.2–4.4 %, suggesting that orientational order in the dispersion can be achieved in dilute dispersions. The experiments on the dispersion with 3.2% iron nanoparticles show that the anisotropy of the scattered intensity is different for the shear-rate-increasing and -decreasing cycles in an applied magnetic field. These results demonstrate entirely different characteristics and orientational distributions for the field-induced orientational order compared to the case of shear-induced orientational order in the dispersions.

ACKNOWLEDGMENTS

Oak Ridge National Laboratory is managed by UT-Battelle, LLC, for the U.S. Department of Energy under Contract No. DE-AC05-00OR22725. This project was supported by United States Department of Energy through Grant No. DE-FG02-02ER45966 and National Science Foundation Materials Research Science and Engineering Center program through Grant No. DMR-0213985. This work was also based in part on activities supported by the National Science Foundation under Agreement No. DMR-9986442.

[1] E. Blums, A. Cebers, and M. N. Maiorov, *Magnetic Fluids* (de Gruyters, New York, 1997).
[2] *Magnetic Fluids and Applications Handbook*, edited by B. M. Berkovsky, Begell House, New York, 1996).
[3] V. V. Krishnamurthy, A. S. Bhandar, M. Piao, I. Zoto, A. M. Lane, D. E. Nikles, J. M. Wiest, G. J. Mankey, L. Porcar, and C. J. Glinka, Phys. Rev. E **67**, 051406 (2003).
[4] R. G. Larson, *The Structure and Rheology of Complex Fluids* (Oxford University Press, New York, 1999).
[5] L. B. Chen, C. F. Zukoski, B. J. Ackerson, H. J. M. Hanley, G. C. Straty, J. Barker, and C. J. Glinka, Phys. Rev. Lett. **69**, 688 (1992).
[6] M. Y. Lin, H. J. M. Hanley, S. K. Sinha, G. C. Straty, D. G. Peiffer, and M. W. Kim, Phys. Rev. E **53**, R4302 (1996).
[7] R. G. Egres, F. Nettesheim, and J. Norman Wagner, J. Rheol. **50**, 685 (2006).
[8] A. S. Bhandar and J. M. Wiest, J. Colloid Interface Sci. **257**, 371 (2003).
[9] A. S. Bhandar, M. Piao, A. M. Lane, and J. M. Wiest, J. Colloid Interface Sci. **268**, 246 (2003).
[10] G. C. Straty, C. D. Muzny, B. D. Butler, M. Y. Lin, T. M. Slawecki, C. J. Glinka, and H. J. M. Henley, Nucl. Instrum. Methods Phys. Res. A **408**, 511 (1998).
[11] S. R. Kline, J. Appl. Crystallogr. **39**, 895 (2006).
[12] W. Wagner, A. Wiedenmann, W. Petry, A. Geibel, and H. Gleiter, J. Mater. Res. **6**, 2305 (1991).
[13] C. G. Shull and M. K. Wilkinson, Phys. Rev. **97**, 304 (1955).
[14] S. M. King, in *Applications of Neutron Scattering to Soft Condensed Matter*, edited by B. J. Gahrys (Gordon and Breach, Amsterdam, 2000), pp. 77–105.
[15] A. Guinier and G. Fournet, *Small-Angle Scattering of X-Rays* (John Wiley and Sons, New York, 1955).
[16] M. Kotlarchyk and M.-H. Chen, J. Chem. Phys. **79**, 2461 (1983).
[17] E. Y. Sheu, Phys. Rev. A **45**, 2428 (1992).
[18] J. B. Hayter and J. Penfold, J. Phys. Chem. **88**, 4589 (1984).
[19] J. S. Pedersen and P. S. Schurtenberger, Macromolecules **29**, 7602 (1996).
[20] J. S. Pedersen and P. S. Schurtenberger, J. Appl. Crystallogr. **29**, 646 (1996).
[21] M. T. Truong and L. M. Walker, Langmuir **18**, 2024 (2002).
[22] K. C. Littrell, J. M. Gallas, G. W. Zajac, and P. Thiyagarajan, Photochem. Photobiol. **77**, 115 (2003).
[23] P. Bolhuis and D. Frenkel, J. Chem. Phys. **106**, 666 (1997).
[24] S. V. Savenko and Marjolean Dijkstra, Phys. Rev. E **70**, 011705 (2004).
[25] L. Onsager, Ann. N. Y. Acad. Sci. **627**, 51 (1949).
[26] A. Leadbetter and E. Norris, Mol. Phys. **38**, 669 (1979).
[27] P. Davidson, Prog. Polym. Sci. **21**, 893 (1996).
[28] A. J. Macleod, Math. Comput. Am. Math. Soc. **60**, 735 (1993).
[29] P. G. de Gennes, *The Physics of Liquid Crystals* (Clarendon Press, Oxford, 1974).
[30] A. Cebers, Magnetohydrodynamics **19**, 1 (1983).
[31] K. I. Morozov, Magnetohydrodynamics **23**, 44 (1987).